Neuroscience 170 (2010) 858–864

NANOSTRUCTURE-INITIATOR MASS SPECTROMETRY (NIMS) IMAGING OF BRAIN CHOLESTEROL METABOLITES IN SMITH-LEMLI-OPITZ SYNDROME

G. J. PATTI,[a] L. P. SHRIVER,[b] C. A. WASSIF,[c] H. K. WOO,[a] W. URITBOONTHAI,[a] J. APON,[a] M. MANCHESTER,[b] F. D. PORTER[c] AND G. SIUZDAK[a]*

[a]*Department of Molecular Biology, Scripps Center for Mass Spectrometry, The Scripps, Research Institute, La Jolla, CA 92037, USA*

[b]*The Skaggs School of Pharmacy and Pharmaceutical Sciences, University of California, San Diego, La Jolla, CA 92037, USA*

[c]*Section on Molecular Dysmorphology, Program in Developmental Endocrinology and Genetics, Eunice Kennedy Shriver National Institute of Child Health and Development, National Institutes of Health, Department of Health and Human Services, Building 10, Room 9D42, 10 Center Dr, Bethesda, MD 20892, USA*

Abstract—Cholesterol is an essential component of cellular membranes that is required for normal lipid organization and cell signaling. While the mechanisms associated with maintaining cholesterol homeostasis in the plasma and peripheral tissues have been well studied, the role and regulation of cholesterol biosynthesis in normal brain function and development have proven much more challenging to investigate. Smith–Lemli–Opitz syndrome (SLOS) is a disorder of cholesterol synthesis characterized by mutations of 7-dehydrocholesterol reductase (DHCR7) that impair the reduction of 7-dehydrocholesterol (7DHC) to cholesterol and lead to neurocognitive deficits, including cerebellar hypoplasia and austism behaviors. Here we have used a novel mass spectrometry-based imaging technique called cation-enhanced nanostructure-initiator mass spectrometry (NIMS) for the *in situ* detection of intact cholesterol molecules from biological tissues. We provide the first images of brain sterol localization in a mouse model for SLOS (*Dhcr7*$^{-/-}$). In SLOS mice, there is a striking localization of both 7DHC and residual cholesterol in the abnormally developing cerebellum and brainstem. In contrast, the distribution of cholesterol in 1-day old healthy pups was diffuse throughout the cerebrum and comparable to that of adult mice. This study represents the first application of NIMS to localize perturbations in metabolism within pathological tissues and demonstrates that abnormal cholesterol biosynthesis may be particularly important for the development of these brain regions.

Key words: Smith–Lemli–Opitz syndrome, brain imaging, nanostructure-initiator mass spectrometry, cholesterol, metabolism, mass spectrometry.

*Correspondence to: G. Siuzdak, Department of Molecular Biology, Scripps Center for Mass Spectrometry, The Scripps, Research Institute, La Jolla, CA 92037, USA. Tel: +1-858-784-9415; fax: +1-858-784-9496.
E-mail address: siuzdak@scripps.edu (G. Siuzdak).

Abbreviations: Ag, silver; DHCR7, 7-dehydrocholesterol reductase; NIMS, nanostructure-initiator mass spectrometry; SHH, sonic hedgehog; SLOS, Smith-Lemli-Optiz syndrome; TOF, time-of-flight; 7DHC, 7-dehydrocholesterol.

Cholesterol is an abundant component of all eukaryotic plasma membranes that plays a critical role in the organization of the lipid bilayer and myelin formation, the regulation of cellular signaling proteins, and as a precursor for steroid molecules (Maxfield and Tabas, 2005). Outside of the CNS, cholesterol metabolism is highly regulated by intracellular proteins and specialized lipoproteins that facilitate transport in the blood (Daniels et al., 2009). Within the brain, however, the blood-brain barrier effectively prevents uptake of cholesterol from circulating plasma (Bjorkhem and Meaney, 2004) and therefore de novo synthesis is the primary mechanism for maintaining cholesterol levels, even in the newborn (Dietschy, 2009). Importantly, demands for cholesterol biosynthesis in the brain change significantly throughout life. The myelin sheath is rich in cholesterol and during postnatal development, when myelination is known to proceed rapidly, cholesterol biosynthesis is highest (Liu et al., 2010). Furthermore, abnormal cholesterol biosynthesis and regulation are implicated in a number of neurological disorders including Alzheimer, Parkinson, and Huntington disease (Rajanikant et al., 2007; Bjorkhem et al., in press; Kolsch et al., 2010). However, the regulatory mechanisms associated with maintaining cholesterol homeostasis in the brain are not well understood.

Genetic defects in enzymes responsible for cholesterol biosynthesis have recently been implicated in developmental disorders causing a variety of abnormalities and malformations in newborns (Porter, 2003). These disorders have elucidated new mechanisms for the role of cholesterol in neurological development. Smith–Lemli–Opitz syndrome (SLOS) results from mutation of the 7-dehydrocholesterol reductase (DHCR7) gene (Fitzky et al., 1998; Wassif et al., 1998; Waterham et al., 1998). The enzyme DHCR7 catalyzes the final step in the Kandutsch–Russell cholesterol biosynthetic pathway that reduces the double bond at carbon 7 on 7-dehydrocholesterol (7DHC) or the double bond at carbon 7 on 7-dehydrodesmosterol to form unesterified cholesterol and desmosterol, respectively (Kandutsch and Russell, 1960; Porter, 2008). Desmosterol can then be converted to cholesterol by 3β-hydroxysterol-Δ24 reductase (DHCR24) (Frantz and Schroepfer, 1967; Correa-Cerro and Porter, 2005). SLOS patients are therefore unable to biosynthesize cholesterol, which leads to elevated levels of cholesterol precursors in addition to dramatically decreased levels of cholesterol (Kelley, 1995). The SLOS phenotype is broad but typically includes craniofacial anomalies, growth failure, cerebellular and brainstem hypoplasia, as well as a distinct behav-

0306-4522/10 $ - see front matter
doi:10.1016/j.neuroscience.2010.07.038

ioral phenotype with autistic manifestations (Kelley and Hennekam, 2000; Wassif et al., 2001).

Several pathological mechanisms have been implicated in the development of clinical features characteristic of SLOS that involve both cholesterol deficiency as well as the accumulation of the cholesterol precursor 7DHC (Jiang et al., 2010). These mechanistic studies have greatly benefited from the development of mouse models of SLOS. Mice homozygous for a null mutation of *Dhcr7* (*Dhcr7*$^{-/-}$) have variable craniofacial anomalies, growth retardation, appear weak, and feed poorly (Wassif et al., 2001). As a result, these animals die during the first day of life. Analysis of cholesterol and its precursors by gas chromatography/mass spectrometry has shown that *Dhcr7*$^{-/-}$ mutant pups have greatly reduced cholesterol levels in the brain (less than 500 μg/g of tissue) and levels of 7DHC that are 250-fold and 265-fold higher in isolated cortex and midbrain respectively relative to healthy controls after birth (Wassif et al., 2001). Localization of these metabolites in intact tissues, however, would provide insight into the role of 7DHC and cholesterol in myelin and neuronal development.

Although gas chromatography/mass spectrometry is the traditional method used for the analysis of sterols, this approach requires extraction of sterol compounds from tissue and therefore does not permit high-resolution spatial localization of metabolites within biological samples. While several other mass spectrometric methods for imaging cholesterol have been described, these strategies are limited by sensitivity, ionization-induced fragmentation, and the inability to confirm compound identification with tandem mass spectrometry (Patti et al., 2010). Therefore we used a novel mass spectrometry-based method for imaging sterol metabolites called nanostructure-initiator mass spectrometry (NIMS). NIMS is a surface-based mass spectrometric technique that is well suited for analysis of metabolites (Northen et al., 2007). Unlike matrix-assisted laser desorption (MALDI), NIMS is matrix free and thereby allows detection of low-mass metabolites without background interference from a matrix. Here we used a technical variation of NIMS in which the NIMS surface was coated with $AgNO_3$ prior to brain tissue deposition and subsequent laser desorption/ionization. Excess Ag^+ on the NIMS surface facilitates cationization of cholesterol metabolites and allows for the *in situ* detection of intact sterols (Patti et al., 2010). The experimental approach provides molecular specificity, sensitivity, and resolution for imaging cholesterol metabolites within biological tissues that is not currently available with other methods. Using cation-enhanced NIMS imaging, we examined the localization of cholesterol and its precursors within the brains of SLOS mice.

EXPERIMENTAL PROCEDURES

Animals and tissue preparation

All experiments were conducted in accordance with the National Institutes of Health and the Scripps Research Institute animal care and use guidelines. Heterozygous *Dhcr7*$^{+/-}$ mice were intercrossed, and *Dhcr7*$^{-/-}$ offspring were analyzed by cation-enhanced NIMS during their first day of life. *Dhcr7*$^{+/+}$ liter mates were analyzed as 1-day old controls. Adult mice (6–8 weeks) were obtained from the Scripps Research Institute Rodent Breeding Colony. Mice were deeply anesthetized by isofluorane inhalation and sacrificed by cervical dislocation. Brains were collected, snap frozen in optimal cutting temperature (OCT) embedding medium (Sigma Aldrich, St. Louis, MO, USA) on dry ice, equilibrated to –20 °C, sectioned to 3–5 μm, and deposited on $AgNO_3$-coated NIMS surfaces. All brains were sectioned using a CM1850 cryostat (Leica Microsystems Inc.).

Preparation of NIMS surfaces

A detailed description of the preparation of NIMS surfaces is reported elsewhere (Woo et al., 2008; Patti et al., 2010). In brief, single-side polished p-type (100) silicon wafers (500–550 μm thick) with low resistivity (0.01–0.02 Ω/cm) were cut into 3.3×3.3 cm^2 pieces (Silicon Quest International, Santa Clara, CA, USA). The cut wafers were soaked in piranha solution (2:1 mixture of sulfuric acid and hydrogen peroxide) for 30 min, rinsed with nanopure water, and blown dry with nitrogen gas. Etching was performed by clamping the chips between gold foil in a Teflon chamber that was filled with 25% ethanolic hydrofluoric acid (HF) solution. A platinum loop was immersed in the HF solution to serve as a cathode. Etchings were performed in constant current mode at 300 mA for 30 min using a PowerPack1000 power supply (Bio Rad, Hercules, CA, USA). The etched surfaces were rinsed with methanol and blown dry with nitrogen. NIMS surfaces were then sprayed with $AgNO_3$ solution (concentration of 0.5 mg/mL in 50% methanol) using a fused-silica PicoTip emitter (New Objective, Woburn, MA, USA). A continuous flow of $AgNO_3$ was maintained using a syringe pump set at a 350 μL/h flow rate and spray voltage of +2 kV. After spray deposition, NIMS surfaces were incubated at 90 °C for 5 min before applying the initiator. After 30 min, the surfaces were blown dry and tissues were thaw-mounted 30 min prior to mass spectrometric analysis.

NIMS imaging

All images were acquired using a time-of-flight (TOF) DE-STR (Voyageur) or a TOF/TOF 5800 (Applied Biosystems, Carlsbad, CA, USA) mass spectrometer. A nitrogen laser at 337 nm or Nd:YAG laser at 355 nm was used. Typically, 20–50 laser shots were collected per spectrum. Propafenone and bradykinin fragment 2–9 were used to calibrate the instrument in the low-mass range. Images were acquired using MS Imaging Tool software with a typical resolution of 75×75 μm^2. Data analysis and image reconstruction was performed using BioMap software. Metabolite identifications were determined by mass (Fig. 1) and confirmed by comparing the MALDI-TOF/TOF fragmentation pattern of the ion to that of an authentic model compound (Sigma Aldrich).

RESULTS

Detection of cholesterol metabolites

Using cation-enhanced NIMS, 7DHC and cholesterol were detected from mouse brain tissue as MAg^+ ions with an *m*/*z* of 491.26 and 493.26, respectively. Given that naturally occurring silver is composed of two stable isotopes, ^{107}Ag and ^{109}Ag, the peaks corresponding to 7DHC and cholesterol in the NIMS spectra demonstrate a unique isotopic pattern characterized by a 2 mass-unit separation (Fig. 1B) (Patti et al., 2010). Accordingly, the ^{109}Ag isotopic peak of 7DHC overlaps with the ^{107}Ag isotopic peak of cholesterol. Although the 7DHC and cholesterol contribu-

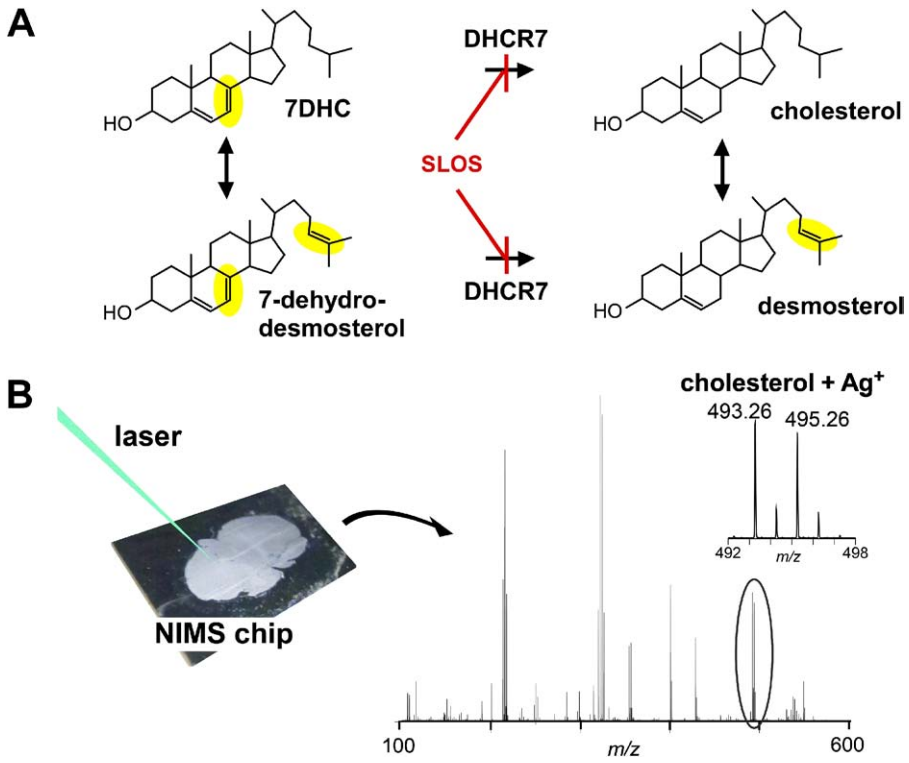

Fig. 1. Application of NIMS to detect cholesterol metabolites dysregulated in SLOS. (A) De novo synthesis of cholesterol. Cholesterol is synthesized from the precursor molecules 7DHC and 7-dehydrodesmosterol. Reduction of the double bond on carbon 7 results in the formation of cholesterol and desmosterol. SLOS involves mutations of DHRC7 that impair reduction of cholesterol precursors. (B) Schematic of cation-enhanced NIMS in which brain sections deposited on $AgNO_3$-coated surfaces are desorbed/ionized by laser irradiation. A typical spectrum acquired from a 3 μm brain section is shown. Silver cationization of cholesterol results in a unique isotopic pattern separated by 2 mass units (inset). For interpretation of the references to color in this figure legend, the reader is referred to the Web version of this article.

tions to peak 493.26 can be readily deconvoluted, the images shown for cholesterol were constructed on the basis of the resolved ^{109}Ag isotopic peak of cholesterol. It is important to emphasize that the relative intensities of each mass spectrometry-based image are independent of one another and cannot be compared between metabolites. For each metabolite, the ion signal with the greatest integrated peak area is assigned a high intensity (red) while the ion signal with the lowest integrated peak area is assigned a low intensity (black).

Distribution of cholesterol metabolites in SLOS mice

Dhcr7$^{-/-}$ animals provide a mouse model of SLOS and show many of the developmental abnormalities seen in human patients (Wassif et al., 2001). We imaged 7DHC and cholesterol in 1-day old *Dhcr7*$^{-/-}$ pups and compared them to healthy, 1-day old controls. In healthy pups, both 7DHC and cholesterol were detected throughout the brain. At this developmental stage myelination has not begun, but it has been established that 1-day old pups synthesize cholesterol de novo for functions that remain unclear (Tint et al., 2006). In control animals the signal intensity of cholesterol was significantly greater than that of 7DHC, consistent with measurements made in healthy animals previously (Wassif et al., 2001). This indicates that 7DHC is readily converted to cholesterol during normal brain development (Fig. 2A–C). In contrast, day 1 SLOS pups show abnormal brain development and a striking localization of significantly increased 7DHC signal in the cerebellum and brainstem (Fig. 2D–F). Although 7DHC was detected throughout the brain of SLOS pups (Fig. 2F, blue area), levels of 7DHC were on average 8-fold higher in the cerebellum and brainstem of all animals analyzed compared to 1-day old controls (Fig. 3A). Consistent with a null mutation, the SLOS pups analyzed in this study have undetectable levels of Dhcr7 activity (Wassif et al., 2001). The residual levels of cholesterol observed in *Dhcr7*$^{-/-}$ pups could be derived from maternal sources or synthesized de novo by an alternative metabolic pathway that has yet to be characterized.

Desmosterol is an intermediate in the synthesis of cholesterol that is known to be present in the brain at higher levels during postnatal development (Kelley and Herman, 2001). Desmosterol and 7DHC are structural isomers that differ only in the location of a carbon-carbon double bond (Fig. 1A). Therefore, desmosterol and 7DHC cannot be resolved with NIMS. SLOS mice, however, cannot synthesize desmosterol as a result of defective *Dhcr7*. For the *Dhcr7*$^{-/-}$ animals used in this study, desmosterol constitutes less than 1% of the total sterols in the brain (Wassif et al., 2001). Thus, the peak at *m*/*z* 491.26 almost

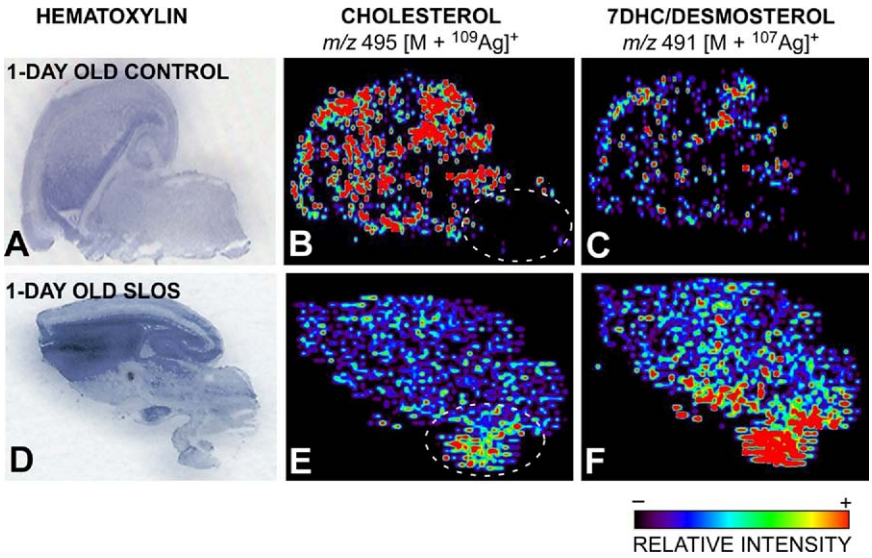

Fig. 2. Hematoxylin staining with corresponding cation-enhanced NIMS images of cholesterol, 7DHC, and/or desmosterol in normal and SLOS pup brains. Images are representative of those obtained from six different animals. (A–C), Images obtained from a control littermate on postnatal day 1. Cholesterol (B) and 7DHC (C) are seen diffusely throughout the cortex. (D–F), Images obtained from *Dhrc*$^{-/-}$ SLOS pups on postnatal day 1. Increased localization of cholesterol (E) and 7DHC (F) is detected in the cerebellum. For interpretation of the references to color in this figure legend, the reader is referred to the Web version of this article.

exclusively results from the accumulation of 7DHC in SLOS mice. For control pups, however, the *m*/*z* 491.26 peak may correspond to either desmosterol or 7DHC.

Imaging of cholesterol in the embryonic Brain

To determine if the localization of sterol metabolites in the hindbrain region of SLOS pups was related to developmental metabolic demands, we evaluated the distribution of cholesterol at embryonic day 16–19 (Fig. 4). In the developing brain of healthy animals, cholesterol is diffuse and does not appear to localize to any specific brain regions that can be resolved with NIMS.

Imaging of cholesterol metabolites in adult mice

In control, adult mice cholesterol and its precursors were distributed throughout the cerebrum (Fig. 5A–C), particularly in the cortex, corpus callosum, and cerebellum. Levels of 7DHC and desmosterol were significantly lower in adult animals relative to 1-day old healthy pups, consistent with the rapid conversion of cholesterol precursors to cholesterol through the action of Dhcr7. The distribution patterns of cholesterol, 7DHC, and desmosterol signal in the 1-day old control pup and adult brains were consistently detected in all animals analyzed, and small areas of increased signal were reproducibly localized to unique regions in both the pup and adult brain. For example, cholesterol metabolites were similarly increased in the hippocampal region of both control pups and adult animals (Fig. 3B). It should be noted that the resolution of both the pup and adult NIMS images are identical, resulting in fewer data points across comparable anatomical features in the smaller pup brain.

DISCUSSION

Cholesterol plays an important role in the development of the CNS that is incompletely understood. It has been suggested that CNS defects related to imbalances in cholesterol homeostasis play a major role in the lethal pathogenesis of *Dhrc7*$^{-/-}$ mice, namely because *Dhrc7*$^{-/-}$ mice have been partially rescued from neonatal death by low-level restoration of Dhcr7 expression in the brain (Yu et al., 2005, 2007). It is well accepted that cholesterol directly regulates a number of signaling systems that may be related to the behavioral and anatomical abnormalities associated with SLOS. However, the mechanisms underlying the physiological changes in the brain that result from disruption of cholesterol biosynthesis are not well understood.

The NIMS images presented here demonstrate that the gene defect in SLOS leads to the accumulation of 7DHC in the developing cerebellum and brainstem. Defects in the development or function of these regions may result from a toxic accumulation of 7DHC that causes disruption of cell function or death (Xu et al., 2010) and/or a lack of cholesterol necessary for membrane organization and the function of key signaling molecules (Jiang et al., 2010). In particular, the signaling factor Sonic hedgehog (SHH) has been identified as a key player in cerebellar development. SHH regulates the proliferation of cerebellar granular neuronal precursors (Hatten et al., 1997), establishing the final number of granular cells and ultimately determining the shape and function of the cerebellum (Vaillant and Monard, 2009). Production of an active SHH signal requires that the protein form a covalent linkage to cholesterol at its C terminus, thereby allowing an active 19 kDa N-terminal fragment that is cleaved during protein

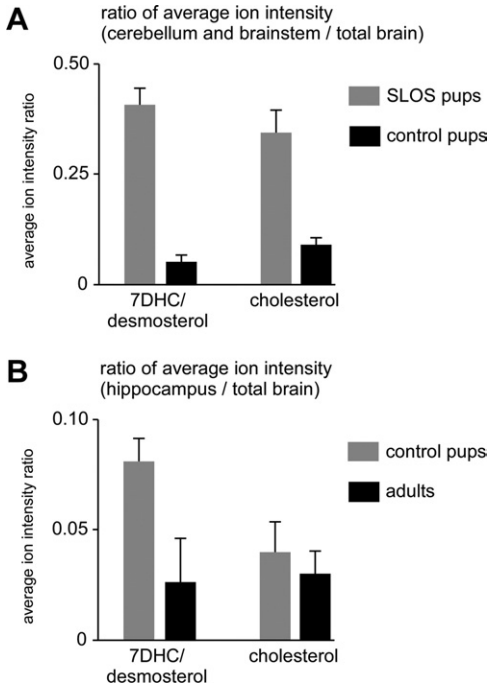

Fig. 3. Relative quantification of cholesterol, 7DHC, and desmosterol in the developing and adult brain. (A) Ratio of average ion intensities from the developing cerebellum and brainstem of 1-day old control (n=3) and SLOS (n=3) pups with respect to the total brain. (B) Ratio of average ion intensities from the hippocampus of 1-day old control pups (n=3) and adult mice (n=3) with respect to the total brain. Data were obtained by taking the ratio of the average ion intensity over the specified brain region (see hashed circles in Fig. 2B, E) with respect to the average ion intensity of the total brain and expressed as ±SEM. The peak corresponding to m/z 491.26 in SLOS pups results almost exclusively from 7DHC and its average ion intensity is approximately 8-fold higher in the developing cerebellum and brainstem relative to its average ion intensity in all other brain regions.

activation to be retained at the cell surface (Porter et al., 1996; Cooper et al., 2003). Therefore, defective SHH signaling from disrupted cholesterol biosynthesis (Lanoue et al., 1997) may be related to the cerebellar pathology observed in SLOS animals.

Regulation of the serotoninergic system by cholesterol may also play an important role in the brain dysfunction of SLOS patients. Autistic manifestations including social and language impairments and repetitive behaviors typical of autism spectrum disorders are common in SLOS patients, estimated to occur in 50–100% of affected individuals, and it has been suggested that SLOS serve as a model to understand the influence of cholesterol homeostasis on autism (Tierney et al., 2001; Sikora et al., 2006; Aneja and Tierney, 2008). Dysfunctional serotonin signaling is one of the most well-replicated neurobiological abnormalities identified in autism (Hanley et al., 1977; Chugani et al., 1997; Buitelaar and Willemsen-Swinkels, 2000; Scott and Deneris, 2005). Interestingly, immunohistochemical data has shown over a 3-fold increase of 5-HT immunoreactivity in the hindbrains of *Dhcr7*$^{-/-}$ mice relative to wild type controls that corresponds to a larger number of 5-HT neurons in SLOS animals (Waage-Baudet et al., 2003). Cholesterol is known to modulate the serotonin receptor that is responsible for controlling the amount of extracellular 5-HT during neurotransmission. Low cholesterol levels reduce serotonin receptor activity and lead to hyperserotonemia (Scanlon et al., 2001). The accumulation of 7DHC and cholesterol in the *Dhcr7*$^{-/-}$ hindbrain region may represent an increased need of cholesterol biosynthesis for serotoninergic regulation.

An alternative mechanism for the cerebellar and brainstem pathology resulting from DHRC7 disruption is the accumulation of 7DHC leading to cell toxicity. SLOS patients display hypocellularity of the brainstem and cerebellum and this may be due to toxic effects of 7DHC on neurons or glia. One-day old SLOS pups show a striking increase in 7DHC when compared to wild type pups. Modification of 7DHC by peroxidation reactions has been shown to result in metabolites that induce apoptosis in neurons (Xu et al., 2010). Additionally, an altered 7DHC/cholesterol ratio is known to affect the function of transcription factors involved in lipid metabolism in a neuronal cell line (Korade et al., 2009). Moreover, administration of the DHRC7 inhibitor AY9944 to 5-day old rats results in increased 7DHC levels, increased lysosomal enzymes, and oligodendrocyte cell death (Igarashi et al., 1975). Our results therefore suggest a correlation between the loss of cells in the cerebellum and brainstem with increased levels of 7DHC in these areas.

Previously, *Dhcr7*$^{-/-}$ mice have been analyzed to identify the relative amount of cholesterol in brain, lung, and liver tissues that is transferred from the mother during development (Tint et al., 2006). Given that *Dhcr7*$^{-/-}$ mothers are heterozygous with a normal level of cholesterol and low level of 7DHC, the assumption of this study is that residual cholesterol in the SLOS pup is exclusively of maternal origin. Applying the same logic, our results allow for the localization of maternally transferred cholesterol within the brain. Interestingly, residual cholesterol colocalizes with 7DHC accumulation in the cerebellum and brainstem of SLOS pups. The relatively low levels of cholesterol

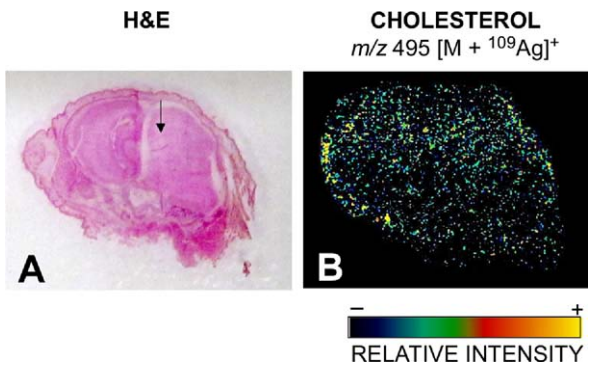

Fig. 4. NIMS imaging of cholesterol in embryonic mouse brain. (A) Hematoxylin and eosin staining that corresponds to the cation-enhanced NIMS image of cholesterol in a day E16–E19 embryo. The embryonic brain is indicated with a black arrow. (B) NIMS image of cholesterol in a day E16–E19 embryo. During late embryonic development the distribution of cholesterol in the brain is diffuse and does not appear to localize to any specific regions that can be resolved in the NIMS image. For interpretation of the references to color in this figure legend, the reader is referred to the Web version of this article.

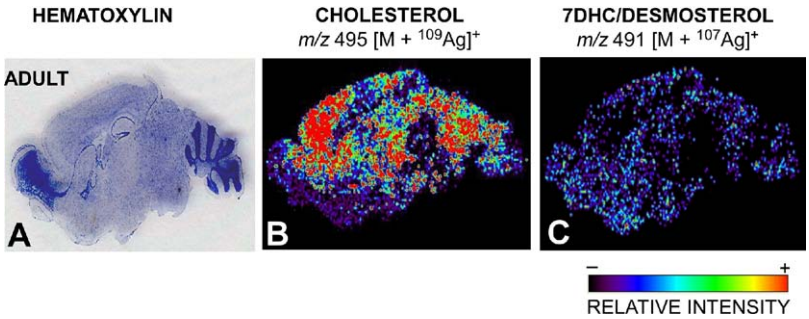

Fig. 5. Hematoxylin staining with corresponding cation-enhanced NIMS images of cholesterol, 7DHC, and/or desmosterol in adult mouse brain. Images are representative of those obtained from three different animals. (A–C), Images obtained from a healthy, adult mouse 6–8 wk of age. The distribution of cholesterol (B) and 7DHC (C) is diffuse throughout the brain, similar to that of healthy pups. For interpretation of the references to color in this figure legend, the reader is referred to the Web version of this article.

within these same regions of healthy 1-day old pups (Fig. 3A) and the absence of accumulated cholesterol within specific regions of the brain late in embryonic development (Fig. 4), however, suggest that the localization of sterol metabolites in SLOS pups is pathological and generally not indicative of normal developmental cholesterol demands.

CONCLUSION

The work described here represents the first application of NIMS to localize perturbations in metabolism within pathological tissues. The capacity to image metabolites provides an opportunity to examine the most down stream end products of cellular reactions that closely correlate with disease phenotype and is therefore likely to provide profound insights into pathological processes. The deposition of cationization agents to the NIMS surface allows for imaging of sterol molecules such as cholesterol, compounds that are notoriously challenging to detect with traditional methods. The application of this technique to SLOS pups has allowed for the localization of cholesterol and its precursors to the developing cerebellum and brainstem region of the brain. The results suggest a role for cholesterol metabolites in the development of these brain regions and provide anatomical insight into the SLOS disease pathology.

Acknowledgments—This work was supported by the California Institute of Regenerative Medicine (TR1-01219), the National Institutes of Health (R24 EY017540-04, P30 MH062261-10, and P01 DA026146-02), NIH/NCRR/STSI UL1 RR025774, the intramural research program of the Eunice Kennedy Shriver National Institute of Child Health and Human Development, and NIH/NINDS 1 F32 NS068015-01A1 (LPS).

REFERENCES

Aneja A, Tierney E (2008) Autism: the role of cholesterol in treatment. Int Rev Psychiatry 20:165–170.

Bjorkhem I, Leoni V, Meaney S (in press) Genetic connections between neurological disorders and cholesterol metabolism. J Lipid Res, in press.

Bjorkhem I, Meaney S (2004) Brain cholesterol: long secret life behind a barrier. Arterioscler Thromb Vasc Biol 24:806–815.

Buitelaar JK, Willemsen-Swinkels SH (2000) Autism: current theories regarding its pathogenesis and implications for rational pharmacotherapy. Paediatr Drugs 2:67–81.

Chugani DC, Muzik O, Rothermel R, Behen M, Chakraborty P, Mangner T, da Silva EA, Chugani HT (1997) Altered serotonin synthesis in the dentatothalamocortical pathway in autistic boys. Ann Neurol 42:666–669.

Cooper MK, Wassif CA, Krakowiak PA, Taipale J, Gong R, Kelley RI, Porter FD, Beachy PA (2003) A defective response to Hedgehog signaling in disorders of cholesterol biosynthesis. Nat Genet 33:508–513.

Correa-Cerro LS, Porter FD (2005) 3beta-hydroxysterol Delta7-reductase and the Smith-Lemli-Opitz syndrome. Mol Genet Metab 84:112–126.

Daniels TF, Killinger KM, Michal JJ, Wright RW Jr, Jiang Z (2009) Lipoproteins, cholesterol homeostasis and cardiac health. Int J Biol Sci 5:474–488.

Dietschy JM (2009) Central nervous system: cholesterol turnover, brain development and neurodegeneration. Biol Chem 390:287–293.

Fitzky BU, Witsch-Baumgartner M, Erdel M, Lee JN, Paik YK, Glossmann H, Utermann G, Moebius FF (1998) Mutations in the Delta7-sterol reductase gene in patients with the Smith-Lemli-Opitz syndrome. Proc Natl Acad Sci U S A 95:8181–8186.

Frantz ID Jr, Schroepfer GJ Jr (1967) Sterol biosynthesis. Annu Rev Biochem 36:691–726.

Hanley HG, Stahl SM, Freedman DX (1977) Hyperserotonemia and amine metabolites in autistic and retarded children. Arch Gen Psychiatry 34:521–531.

Hatten ME, Alder J, Zimmerman K, Heintz N (1997) Genes involved in cerebellar cell specification and differentiation. Curr Opin Neurobiol 7:40–47.

Igarashi M, Suzuki K, Chen SM (1975) Changes in brain hydrolytic enzyme activities in rats treated with cholesterol biosynthesis inhibitor, AY9944. Brain Res 90:97–114.

Jiang XS, Wassif CA, Backlund PS, Song L, Holtzclaw LA, Li Z, Yergey AL, Porter FD (2010) Activation of Rho GTPases in Smith-Lemli-Opitz syndrome: pathophysiological and clinical implications. Hum Mol Genet 19:1347–1357.

Kandutsch AA, Russell AE (1960) Preputial gland tumor sterols. 3. A metabolic pathway from lanosterol to cholesterol. J Biol Chem 235:2256–2261.

Kelley RI (1995) Diagnosis of Smith-Lemli-Opitz syndrome by gas chromatography/mass spectrometry of 7-dehydrocholesterol in plasma, amniotic fluid and cultured skin fibroblasts. Clin Chim Acta 236:45–58.

Kelley RI, Hennekam RC (2000) The Smith-Lemli-Opitz syndrome. J Med Genet 37:321–335.

Kelley RI, Herman GE (2001) Inborn errors of sterol biosynthesis. Annu Rev Genomics Hum Genet 2:299–341.

Kolsch H, Heun R, Jessen F, Popp J, Hentschel F, Maier W, Lutjohann D (2010) Alterations of cholesterol precursor levels

in Alzheimer's disease. Biochim Biophys Acta 1801:945–950.

Korade Z, Kenworthy AK, Mirnics K (2009) Molecular consequences of altered neuronal cholesterol biosynthesis. J Neurosci Res 87: 866–875.

Lanoue L, Dehart DB, Hinsdale ME, Maeda N, Tint GS, Sulik KK (1997) Limb, genital, CNS, and facial malformations result from gene/environment-induced cholesterol deficiency: further evidence for a link to sonic hedgehog. Am J Med Genet 73:24–31.

Liu JP, Tang Y, Zhou S, Toh BH, McLean C, Li H (2010) Cholesterol involvement in the pathogenesis of neurodegenerative diseases. Mol Cell Neurosci 43:33–42.

Maxfield FR, Tabas I (2005) Role of cholesterol and lipid organization in disease. Nature 438:612–621.

Northen TR, Yanes O, Northen MT, Marrinucci D, Uritboonthai W, Apon J, Golledge SL, Nordstrom A, Siuzdak G (2007) Clathrate nanostructures for mass spectrometry. Nature 449:1033–1036.

Patti GJ, Woo HK, Yanes O, Shriver L, Thomas D, Uritboonthai W, Apon JV, Steenwyk R, Manchester M, Siuzdak G (2010) Detection of carbohydrates and steroids by cation-enhanced nanostructure-initiator mass spectrometry (NIMS) for biofluid analysis and tissue imaging. Anal Chem 82:121–128.

Porter FD (2003) Human malformation syndromes due to inborn errors of cholesterol synthesis. Curr Opin Pediatr 15:607–613.

Porter FD (2008) Smith-Lemli-Opitz syndrome: pathogenesis, diagnosis and management. Eur J Hum Genet 16:535–541.

Porter JA, Young KE, Beachy PA (1996) Cholesterol modification of hedgehog signaling proteins in animal development. Science 274:255–259.

Rajanikant GK, Zemke D, Kassab M, Majid A (2007) The therapeutic potential of statins in neurological disorders. Curr Med Chem 14:103–112.

Scanlon SM, Williams DC, Schloss P (2001) Membrane cholesterol modulates serotonin transporter activity. Biochemistry 40:10507–10513.

Scott MM, Deneris ES (2005) Making and breaking serotonin neurons and autism. Int J Dev Neurosci 23:277–285.

Sikora DM, Pettit-Kekel K, Penfield J, Merkens LS, Steiner RD (2006) The near universal presence of autism spectrum disorders in children with Smith-Lemli-Opitz syndrome. Am J Med Genet A 140:1511–1518.

Tierney E, Nwokoro NA, Porter FD, Freund LS, Ghuman JK, Kelley RI (2001) Behavior phenotype in the RSH/Smith-Lemli-Opitz syndrome. Am J Med Genet 98:191–200.

Tint GS, Yu H, Shang Q, Xu G, Patel SB (2006) The use of the Dhcr7 knockout mouse to accurately determine the origin of fetal sterols. J Lipid Res 47:1535–1541.

Vaillant C, Monard D (2009) SHH pathway and cerebellar development. Cerebellum 8:291–301.

Waage-Baudet H, Lauder JM, Dehart DB, Kluckman K, Hiller S, Tint GS, Sulik KK (2003) Abnormal serotonergic development in a mouse model for the Smith-Lemli-Opitz syndrome: implications for autism. Int J Dev Neurosci 21:451–459.

Wassif CA, Maslen C, Kachilele-Linjewile S, Lin D, Linck LM, Connor WE, Steiner RD, Porter FD (1998) Mutations in the human sterol delta7-reductase gene at 11q12-13 cause Smith-Lemli-Opitz syndrome. Am J Hum Genet 63:55–62.

Wassif CA, Zhu P, Kratz L, Krakowiak PA, Battaile KP, Weight FF, Grinberg A, Steiner RD, Nwokoro NA, Kelley RI, Stewart RR, Porter FD (2001) Biochemical, phenotypic and neurophysiological characterization of a genetic mouse model of RSH/Smith-Lemli-Opitz syndrome. Hum Mol Genet 10:555–564.

Waterham HR, Wijburg FA, Hennekam RC, Vreken P, Poll-The BT, Dorland L, Duran M, Jira PE, Smeitink JA, Wevers RA, Wanders RJ (1998) Smith-Lemli-Opitz syndrome is caused by mutations in the 7-dehydrocholesterol reductase gene. Am J Hum Genet 63:329–338.

Woo HK, Northen TR, Yanes O, Siuzdak G (2008) Nanostructure-initiator mass spectrometry: a protocol for preparing and applying NIMS surfaces for high-sensitivity mass analysis. Nat Protoc 3:1341–1349.

Xu L, Korade Z, Porter NA (2010) Oxysterols from free radical chain oxidation of 7-dehydrocholesterol: product and mechanistic studies. J Am Chem Soc 132:2222–2232.

Yu H, Li M, Tint GS, Chen J, Xu G, Patel SB (2007) Selective reconstitution of liver cholesterol biosynthesis promotes lung maturation but does not prevent neonatal lethality in Dhcr7 null mice. BMC Dev Biol 7:27.

Yu H, Wessels A, Tint GS, Patel SB (2005) Partial rescue of neonatal lethality of Dhcr7 null mice by a nestin promoter-driven DHCR7 transgene expression. Brain Res Dev Brain Res 156:46–60.

(Accepted 18 July 2010)
(Available online 27 July 2010)